2012

HLH-29 Regulates Ovulation in C. Elegans by Targeting Genes in the Inositol Triphosphate Signaling Pathway

Casonya Johnson
Georgia State University, cjohnson113@gsu.edu

Ana White
Georgia State University

Abegail Fearon
Georgia State University

HLH-29 regulates ovulation in *C. elegans* by targeting genes in the inositol triphosphate signaling pathway

Ana White[1], Abegail Fearon[1] and Casonya M. Johnson[1,*]

[1]Department of Biology, College of Arts and Sciences, Georgia State University, Atlanta, GA 30303, USA

*Author for correspondence (cjohnson113@gsu.edu)

Biology Open 1, 261–268
doi: 10.1242/bio.2012046

Summary

The reproductive cycle in the nematode *Caenorhabditis elegans* depends in part on the ability of the mature oocyte to ovulate into the spermatheca, fuse with the sperm during fertilization, and then exit the spermatheca as a fertilized egg. This cycle requires the integration of signals between the germ cells and the somatic gonad and relies heavily on the precise control of inositol 1,4,5 triphosphate (IP_3)levels. The HLH-29 protein, one of five Hairy/Enhancer of Split (HES) homologs in *C. elegans,* was previously shown to affect development of the somatic gonad. Here we show that HLH-29 expression in the adult spermatheca is strongly localized to the distal spermatheca valve and to the spermatheca-uterine valve, and that loss of *hlh-29* activity interferes with oocyte entry into and egg exit from the spermatheca. We show that HLH-29 can regulate the transcriptional activity of the IP_3 signaling pathway genes *ppk-1*, *ipp-5*, and *plc-1* and provide evidence that *hlh-29* acts in a genetic pathway with each of these genes. We propose that the HES-like protein HLH-29 acts in the spermatheca of larval and adult animals to effectively increase IP_3 levels during the reproductive cycle.

Key words: Hairy/enhancer of split, Transcriptional regulation, Spermatheca-uterine valve, Somatic gonad

Introduction

The basic helix loop helix (bHLH) transcription factors are critical regulators of early development (Maroto et al., 2008; Barnes and Firulli, 2009; Egoz-Matia et al., 2011), with roles in regulating organogenesis and neurosensory development (Pin et al., 2001; Ligon et al., 2006; Zhao et al., 2006; Du and Yip, 2011). Members of the Hairy-Enhancer of Split (HES) subfamily act primarily in response to Notch signaling (Fischer and Gessler, 2007; Kageyama et al., 2007), and are known for roles in neural (Kageyama et al., 2008; Li et al., 2008; Webb et al., 2011) and cardiovascular (Fischer et al., 2004; Xin et al., 2007; Wiese et al., 2010) development. In humans, mutations in the HES genes are often associated with neuroblastoma (Axelson, 2004; Stockhausen et al., 2005), neuroendocrine tumors of the breast, lung, and prostate (Hartman et al., 2009; Lu et al., 2010; Nasgashio et al., 2011), and early developmental disorders (Sparrow et al., 2008; Sparrow et al., 2010). While members of the bHLH superfamily are also needed post-embryonically for metamorphosis (Lo et al., 2007; Parthasarathy et al., 2008; Bitra et al., 2009), sexual development and gamete formation (Van Wayenbergh et al., 2003; Ballow et al., 2006; Lu et al., 2008), and maintaining homeostasis (Zhou et al., 2009; Li et al., 2010; Long et al., 2010), little is known about the post-embryonic, non-developmental roles of the HES family proteins.

Ovulation in *Caenorhabditis elegans* is a tightly regulated process that demonstrates how cells and tissues must coordinate major signaling events to function. Critical to the ovulation cycle are a series of communication events between the proximal oocyte and sperm, and between the gametes and the surrounding sheath cells of the somatic gonad (Han et al., 2010; see Fig. 1). After receiving molecular signals from the sperm, the proximal oocyte undergoes maturation and sends its own signal to the gonadal sheath cells to amplify contractions that were initiated by the sperm-derived signals (Greenstein, 2005; Govindan et al., 2006). These oocyte-derived signals, which include the *C. elegans* epidermal growth factor homolog, LIN-3, also activate the dilation of the distal spermatheca valve. Ovulation occurs when the oocyte is propelled into the spermatheca. Sheath cell contractions, dilation of the distal spermatheca valve, and dilation of the spermatheca-uterine (SP-UT) valve after fertilization all require intracellular calcium release that is induced by LIN-3 dependent, inositol triphosphate (IP_3) signaling in the spermatheca and sheath cells (Clandinin et al., 1998; Bui and Sternberg, 2002; Yin et al., 2004). Here we show that the HES-like protein HLH-29 controls spermatheca entry and exit by altering the expression of genes required for IP_3 signaling, thereby providing one of the first links between a HES protein and the coordination of a rhythmic post-embryonic biological process.

Materials and Methods

Nematode handling and strains

The following strains were used: N2 Bristol wild-type (Brenner, 1974); TM284, *hlh-29(tm284)*; SL232, *unc-51*(e1189) *fog-2(q71)*/*fog-2*(q71) *rol-9(sc148)*; PS2286, *unc-38(x20) lfe-2(sy326)*; PS3656, *ipp-5(sy605)*. Transgenic lines carrying an integrated *hlh-29*::GFP transgene were previously described (McMiller et al., 2007). Culture growth and synchronization by alkaline hypochlorite treatment were as previously described (Lewis and Fleming, 1995).

Brood Size and Epistasis Analysis

Animals were raised for at least two generations at 22℃ prior to the start of assays, and were fed bacteria producing dsRNA for either the control gene *unc-55* or for

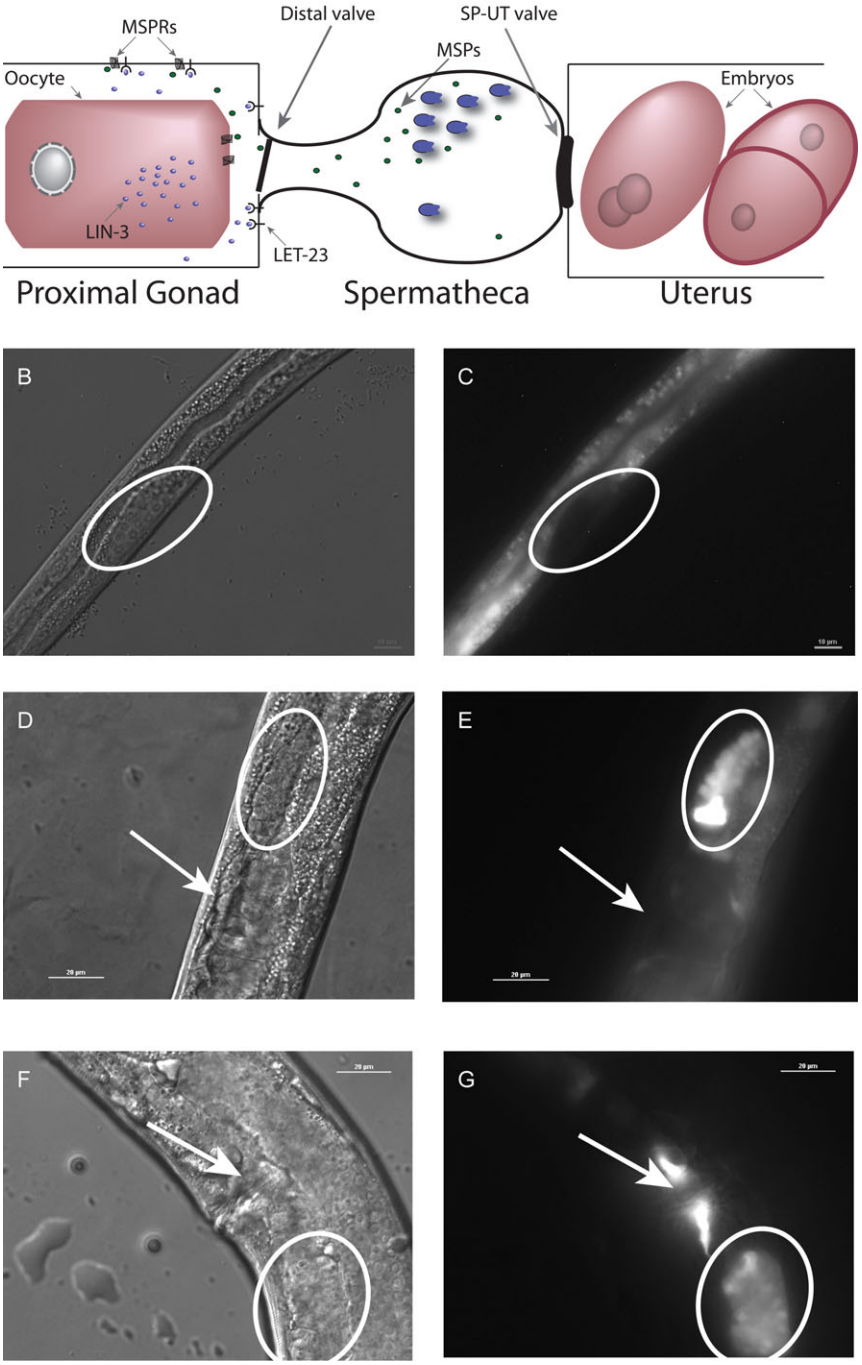

Fig. 1. HLH-29 is expressed in the adult spermatheca during ovulation. (A) Ovulation in wild-type animals is stimulated when major sperm (MSP) proteins bind to receptors on the proximal oocyte and the proximal gonad to stimulate meiotic maturation and gonad contractions, respectively. The oocyte then secretes LIN-3 protein, which binds to the receptor protein LET-23 and amplifies the gonad contractions. LET-23 activation also triggers the dilation of the distal spermatheca valve. The oocyte is propelled into the spermatheca, where it is fertilized and subsequently expelled through the SP-UT valve into the uterus. **(B–G)** *hlh-29*::GFP expression in the spermatheca of animals bearing an integrated transcriptional reporter construct. Corresponding DIC images are shown on the left of each epifluorescence micrograph. (B,C) Lateral view, L2/L3 stage. Cells of the somatic primordium are circled. (D,E) Dorsal view, early L4 stage. Anterior spermatheca is circled; arrow indicates uterus and vulval lumen. (F,G) Lateral view, adult stage. Posterior spermatheca is circled; arrow indicates vulva muscles.

the test genes (Kamath and Ahringer, 2003). It should be noted that because *hlh-28* and *hlh-29* produce identical mRNAs, RNAi against *hlh-29* mRNA also knocks down *hlh-28* mRNA. Therefore, the RNAi effects described here may be the result of knockdown of both *hlh-28* and *hlh-29* and we will refer to this treatment as *hlh-29/hlh-28* RNAi. For brood size assays and for ovulation assays with *fog-2* animals, L4 stage hermaphrodites were serially transferred to fresh plates every 24 hours throughout their egg laying period. For epistasis analysis, L1 stage animals were fed control bacteria for 56 hours at 22.5℃ and then moved, individually, to 35 mm NGM plates seeded with bacteria producing the appropriate dsRNA. Eggs and oocytes were counted twice: when the adult hermaphrodite was first removed from the plates, and again 24 hours later. The data are presented as the number of viable progeny (brood size), and oocyte percentage (number oocytes/(number oocytes + viable progeny). Inviable and abnormally shaped eggs were eliminated because we could not consistently differentiate between fragmented eggs and fragmented oocytes. Finally, the *hlh-29(tm284)* animals used for these assays were homozygous for the tm284 allele.

Time-lapse Microscopy

Animals were anesthetized with 0.1% levamisole (Govindan et al., 2009), mounted on 2.0% agarose pads and imaged using a 60X oil-immersion objective with a Nikon Eclipse 90i microscope equipped with a Nikon Coolsnap CCD camera.

Images were captured at 3 second intervals over a 115 minute period using NIS-elements, version 3.2 software (Nikon). Audio video interleave (AVI) files were generated by NIS-elements and compressed using H.264, then exported as moving picture experts group, standard 4 (MPEG-4) movies using Xilisoft Video Converter Ultimate, Version 6.0.7. Because ovulation occurred sporadically in *hlh-29(tm284)* homozygous animals due in part to variable defects in the gonad morphology, we used *hlh-29/hlh-28* RNAi treated *hlh-29(tm284)* heterozygotes to capture ovulation by time lapse microscopy.

Gene Expression Analysis

Gene expression analysis, including total RNA extraction, cDNA synthesis, and real-time PCR were carried out as previously described (Felton and Johnson, 2011). Total RNA was extracted from late L4 or early adult stage populations, and cDNA synthesis reactions were performed in 50 µL reaction volumes containing 10.0 µg of total RNA. Real time PCR assays were performed with Taqman Gene Expression Assays (Applied Biosystems) specific for each putative target (supplementary material Table S1), using relative quantitation with normalization against the endogenous control gene *pmp-3* (Hoogewijs et al., 2008).

Egg-laying Measurements

Egg-laying in the presence of food was assayed using synchronized cultures that were fed for 72 hours after hatching at 22℃. Two hermaphrodites were placed onto seeded, 35 mm NGM plates and incubated at 22℃. After two hours, the number of eggs and unfertilized oocytes were counted. Animals that did not produce progeny or who ruptured through vulva (exp) during the assay were excluded. For this assay N=30; each experiment was repeated in triplicate.

For egg laying assays in the absence of food, each culture of L1 stage animals was fed bacteria producing the appropriate dsRNA for 72 hours. Animals were then picked onto an unseeded NGM plate and allowed to crawl around for 30 minutes so that all bacteria could be removed from their bodies. Hermaphrodites were then placed individually into each well of a 48-well tissue culture plate containing 25 µL of M9 buffer, and incubated at 22℃ for 1 hour. Animals that ruptured through the vulva while in buffer or that displayed anatomical defects were excluded from the assay. For this assay, N=288; each experiment was repeated 5 times.

Results and Discussion

HLH-29 is expressed in the spermatheca and plays a role in egg-laying

Previously, we reported that RNAi knockdown of *hlh-29* and the duplicate gene *hlh-28* results in the exploded through vulva (exp), protruding vulva (pvl), and accumulated endomitotic oocytes (emo) phenotypes (McMiller et al., 2007). Additionally, a fraction of RNAi animals failed to form a uterus, failed to develop one of the two gonad arms, or accumulated either unfertilized or emo oocytes in the uterus. These phenotypes are also evident in animals that carry null alleles of either *hlh-29* or *hlh-28*. Both *hlh-29* and *hlh-28* are expressed in all cells of the EMS lineage in early embryos (Broitman-Maduro et al., 2005; Neves and Priess, 2005). The post-embryonic expression pattern of *hlh-28* is unknown; however an *hlh-29*::GFP transcriptional reporter is expressed in cells of MS descendants that give rise to the adult spermatheca and vulva muscles (McMiller et al., 2007). Together, these data suggest a pleiotropic role for HLH-29 and HLH-28 in reproduction. We sought to better understand the role of HLH-29 in reproduction and we reasoned that any functional differences between the identical proteins HLH-29 and HLH-28 would be due solely to differences in timing and location of expression. It should be noted, however, that because *hlh-29* and *hlh-28* are identical genes, with the exception of an additional exon in *hlh-28* that is believed to be removed via splicing (McMiller et al., 2007), RNAi knockdown of *hlh-29* also results in knockdown of *hlh-28*. This raises the possibility that the RNAi phenotypes described below may be the result of reduction in the activities of both genes.

hlh-29 is expressed in most cells of the spermatheca of L4 and adult animals, and in the vulva muscles, but not in the spermatheca or vulval precursor cells of younger animals (Fig. 1). Unlike in wild-type animals, egg-laying rates in *hlh-29(tm284)* animals are not responsive to changes in food availability (supplementary material Fig. S1), and more interestingly, *hlh-29(tm284)* animals lay unfertilized oocytes throughout their egg-laying period. Most of these unfertilized oocytes were endomitotic, as indicated by disorganized and enlarged nuclei (Iwasaki et al., 1996); however, *hlh-29(tm284)* animals also lay unfertilized oocytes that have distinct, normal-sized nuclei or that appear to lack a nucleus. To determine whether the unfertilized oocytes phenotype is solely from exhausting the supplies of active sperm or is also the result of defective ovulation cycles, we treated *fog-2(q71)* animals with RNAi against *hlh-29/hlh-28*. *fog-2* animals do not produce sperm and can be used to identify genes that function during ovulation (Govindan et al., 2006). We found that *fog-2(q71)* animals eating either OP50 or bacteria producing control RNAi laid an average of 2.9 oocytes/24 hours at 25℃ (SEM =0.449, n=156), while *fog-2(q71)*; *hlh-29/hlh-28*(RNAi) animals laid an average of 28.73 oocytes/24 hours (SEM =1.345, n=190, p-value $=4.27e^{-19}$). While this result does not rule out the possibility that *hlh-29* affects sperm viability and function, it does support a sperm-independent role for *hlh-29* in regulating reproduction.

Ovulation is defective in *hlh-29* animals

In wild-type animals, each gonad arm ovulates one mature oocyte on average of every 23 minutes. In the oocyte, the events leading up to ovulation include distal nuclear migration, breakdown of the nuclear envelope, and cortical rearrangement. Ovulation itself, the propulsion of the mature oocyte into the spermatheca, requires intense rhythmic contractions of the surrounding gonad sheath cells, followed by dilation or extension of the distal spermatheca valve. In wild-type animals, the ovulated oocyte is fertilized almost immediately, and within five minutes of ovulation, the fertilized egg emerges through the SP-UT valve into the uterus (McCarter et al., 1999).

The morphology of the gonad arms is affected in animals lacking HLH-29 (McMiller et al, 2007), making it difficult to analyze ovulation in *hlh-29(tm284)* homozygous animals. HLH-29′s effect on gonad morphology appears to be dose and developmental stage dependent, and we were able to separate this phenotype from the ovulation phenotype by subjecting L3 stage heterozygous *hlh-29(tm284)* animals, to *hlh-29/hlh-28* RNAi. The ovulation defects were the same in N2 and in *hlh-29(tm284)* heterozygous animals treated with *hlh-29/hlh-28* RNAi, and also in *hlh-29(tm284)* homozygotes. These defects ranged from complete failure of the oocyte to enter the spermatheca to complete failure of the fertilized egg to exit the spermatheca. We found, however, that defective ovulation occurred more frequently in RNAi treated *hlh-29(tm284)* heterozygotes than in N2 animals. Therefore, we used *hlh-29/hlh-28* RNAi treat *hlh-29(tm284)* heterozygotes, referred to henceforth as *hlh-29(tm284)/+ hlh-29/hlh-28*(RNAi) animals, to capture the ovulation defects by time-lapse microscopy.

Distal nuclear migration, breakdown of the nuclear envelope, and cortical rearrangement appeared to occur normally in *hlh-29(tm284)/+ hlh-29/hlh-28*(RNAi) animals, suggesting that HLH-29 is not required for oocyte maturation. This result was unexpected in light of the *fog-2; hlh-29/hlh-28* (RNAi) results described above. Genes previously shown to influence ovulation in *fog-2* animals are believed to negatively regulate meiotic maturation. RNAi knockdown of those genes normally increases maturation rates in unmated *fog-2* females, though not to the same rates as those seen in hermaphrodites or in mated *fog-2*

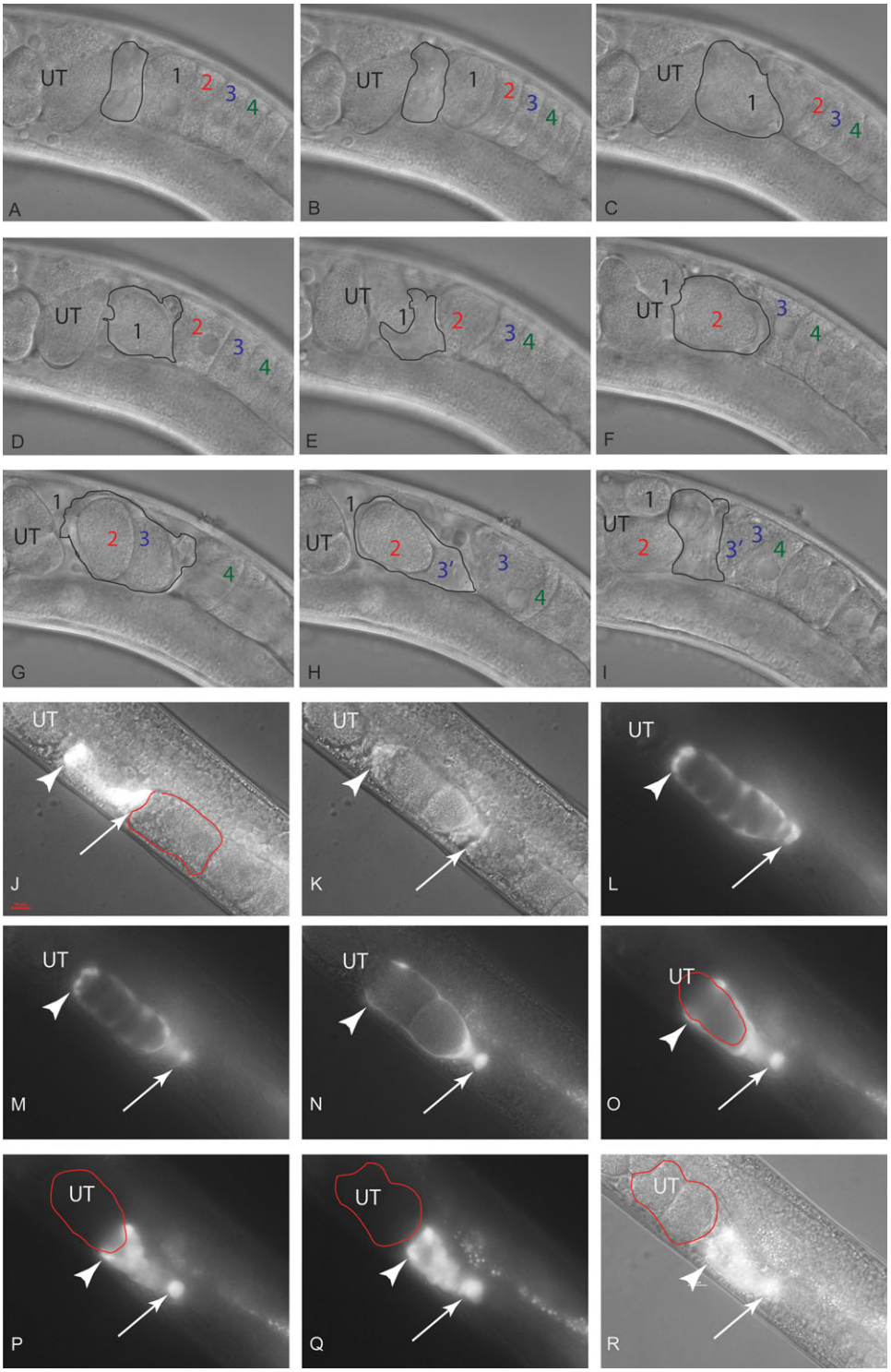

Fig. 2. Time lapse observations of ovulation. (A–I) Representative abnormal ovulation in an *hlh-29(tm284)/+ hlh-29/hlh-28*(RNAi) animal. The spermatheca is outlined in black, the uterus, with developing embryos, is indicated by UT, and the first four oocytes in the gonad arm are numbered. Oocyte 1 enters and exits the spermatheca successfully, but oocyte 2 is not able to exit until oocyte 3 is ovulated. All subsequent ovulations are blocked when oocyte 3 is fragmented (indicated by 3 and 3′) while exiting backwards through the distal valve. **(J–R)** Representative ovulation in an animal carrying the integrated *hlh-29*::GFP transgene. Expression in the spermatheca is concentrated in the distal (white arrow) and the SP-UT valves (arrowhead). The ovulating oocyte (fertilized embryo in P & R) is outlined in red.

females (Govindan et al., 2006). It is possible that HLH-29 and HLH-28 function in different tissues to regulate the expression of two separate sets of genes that are required to separate meiotic maturation and the initiation of ovulation from physical movement through the spermatheca. This possibility would explain why ovulation increases in *fog-2; hlh-29/hlh-28* (RNAi) animals and also may explain why *hlh-29/hlh-28* RNAi rescues the brood size phenotypes of *hlh-29(tm284)* animals (see below).

Loss of HLH-29 did not appear to affect gonadal sheath contractions; however, the ability of oocytes and fertilized eggs to enter and exit the spermatheca, respectively, was affected (supplementary material Movies 1–3). This ovulation defect was highly variable and occurred randomly in either gonad arm. We compared ovulation events over a 90 minute period in wild-type and in *hlh-29(tm284)/+ hlh-29/hlh-28* (RNAi) animals (supplementary material Table S2), and defined a successful

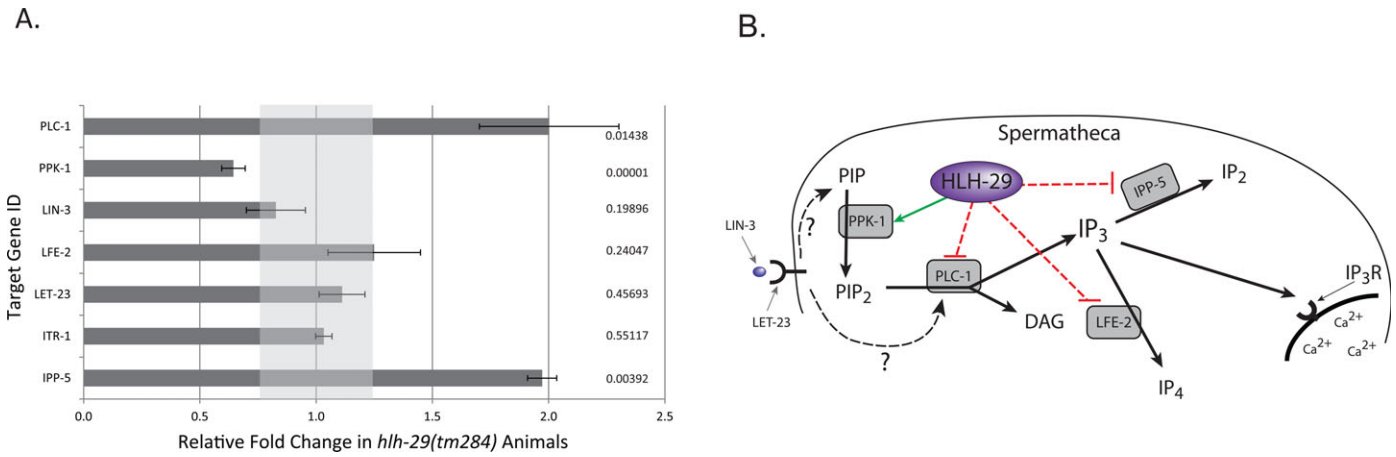

Fig. 3. HLH-29 and the IP_3 signaling. (A) Transcriptional activity of genes in the IP_3 signaling transduction pathway are affected in *hlh-29(tm284)* animals. Bars represent the relative fold-change in mRNA levels as detected by RT-qPCR when compared to expression in wild-type animals, error bars represent standard error of the mean. Fold expression range considered to be the same as wild-type expression is indicated by light gray shading, centered around the value of 1.0. P values are indicated to the right of each bar. **(B)** Components of the LIN-3/LET-23 activated IP_3 signaling transduction pathway are transcriptionally regulated by HLH-29.

event as entry into the spermatheca followed by unassisted exit out of the spermatheca within eight minutes. This eight minute fertilization window is significantly longer than the previously published wild-type fertilization window of two minutes (McCarter et al., 1999), and may have resulted in an underestimation of the number of abnormal ovulation events. We observed a total of 14 ovulation events in a single gonad arm of 4 different wild-type animals; all but one of these events occurred normally, at an average frequency of one every 21.5 minutes. Similarly, N2 animals treated with control RNAi had normal ovulation events that occurred at an average frequency of one every 28 minutes (data not shown).

We observed a total of 46 ovulation events in a single gonad arm of 21 different *hlh-29(tm284)/+ hlh-29/hlh-28* (RNAi) animals, 24 of which occurred normally (supplementary material Table S2). The average frequency of attempted/successful ovulation events in these animals was one every 41 minutes. This average does not include the ovulation attempts made by gonad arms that became blocked within the 90 minute observation period. Failure of either the distal spermatheca valve or the SP-UT valve to function properly resulted in fragmented oocytes and embryos which accumulated in the gonad arms and uterus, or in occupancy of the spermatheca by multiple oocytes (Fig. 2A–I), some of which eventually become emo. In 11 of 21 events, abnormal ovulations were caused by failure of the distal spermatheca valve to function properly. Oocytes failed to enter the spermatheca (8/11), were fragmented upon entry because the valve closed prematurely (2/11), or fell back into the gonad arm (1/11) because the valve failed to close completely (supplementary material Fig. S2A–C). In 7 of 21 events, abnormal ovulations were caused by failure of the SP-UT valve to function properly. The most infrequent failures occurred when the SP-UT valve failed to open at all, resulting in blockage of the spermatheca (1/7) or of the gonad arm (1/7) by a fertilized egg. More often, the fertilized egg exited the spermatheca either unassisted after a prolonged occupancy (1/7), or as a result of entry into the spermatheca by a second oocyte (4/7). The fate of the second oocyte included successfully fertilized and ovulated (1), fragmented exit into the uterus (1/4), forced exit into the gonad arm (1/4), and rapid exit into the uterus without fertilization (1/4). Taken together, defective ovulation in *hlh-29(tm284)/+ hlh-29/hlh-28*(RNAi) animals appears to be the result of mechanical failure of both of the spermatheca valves.

Consistent with this mechanical failure, *hlh-29* activity localized to both the distal and proximal valves of the spermatheca (Fig. 2J-R; supplementary material Movie 4). Together, these results suggest that HLH-29 is required to allow successful entry into and exit from the spermatheca.

HLH-29 acts as a positive and a negative regulator of genes expressed in the adult spermatheca

We tested the effect of loss of *hlh-29* activity on genes whose expression overlapped with *hlh-29* in the spermatheca and that were previously shown to affect ovulation. We found that loss of HLH-29 reduced the activity of *ppk-1* and increased the activities of *plc-1* and *ipp-5* (Fig. 3A), three genes required for IP_3 signaling. Loss of HLH-29 also caused a 1.3 fold increase in *lfe-2* activity, though this change was not found to be statistically significant.

We looked for genetic interactions between *hlh-29* and *ppk-1*, *ipp-5*, and *lfe-2* using measurements of brood size and percentage of unfertilized oocytes (see methods and materials). *ppk-1* encodes a kinase that converts phosphatidylinositol-4-phosphate (PIP) into phosatidylinositol 4, 5-bisphosphate (PIP_2), which is subsequently hydrolyzed by phospholipase C into the second messengers diacylglycerol (DAG) and inositol 1,4,5-triphosphate (IP_3) (Fig. 3B). Loss of PPK-1 causes the accumulation of oocytes in the gonad arms due, in part, to the absence of gonadal sheath contractions during ovulation (Xu et al., 2007). Feeding newly hatched N2 or homozygous *hlh-29(tm284)* animals bacteria producing *ppk-1*dsRNA resulted in 100% sterility (not shown). We found that N2 and *hlh-29(tm284)* animals that received *ppk-1* RNAi after L3 stage produced almost as many viable progeny as those that were subjected to control RNAi (Fig. 3B) during the same time period, and so we used these animals for the epistasis assays. Wild-type animals laid a small percentage of unfertilized oocytes at the end of their egg-laying period (Fig. 4A), but this percentage was reduced in *ppk-1* (RNAi) animals. *hlh-29(tm284)* animals laid unfertilized oocytes

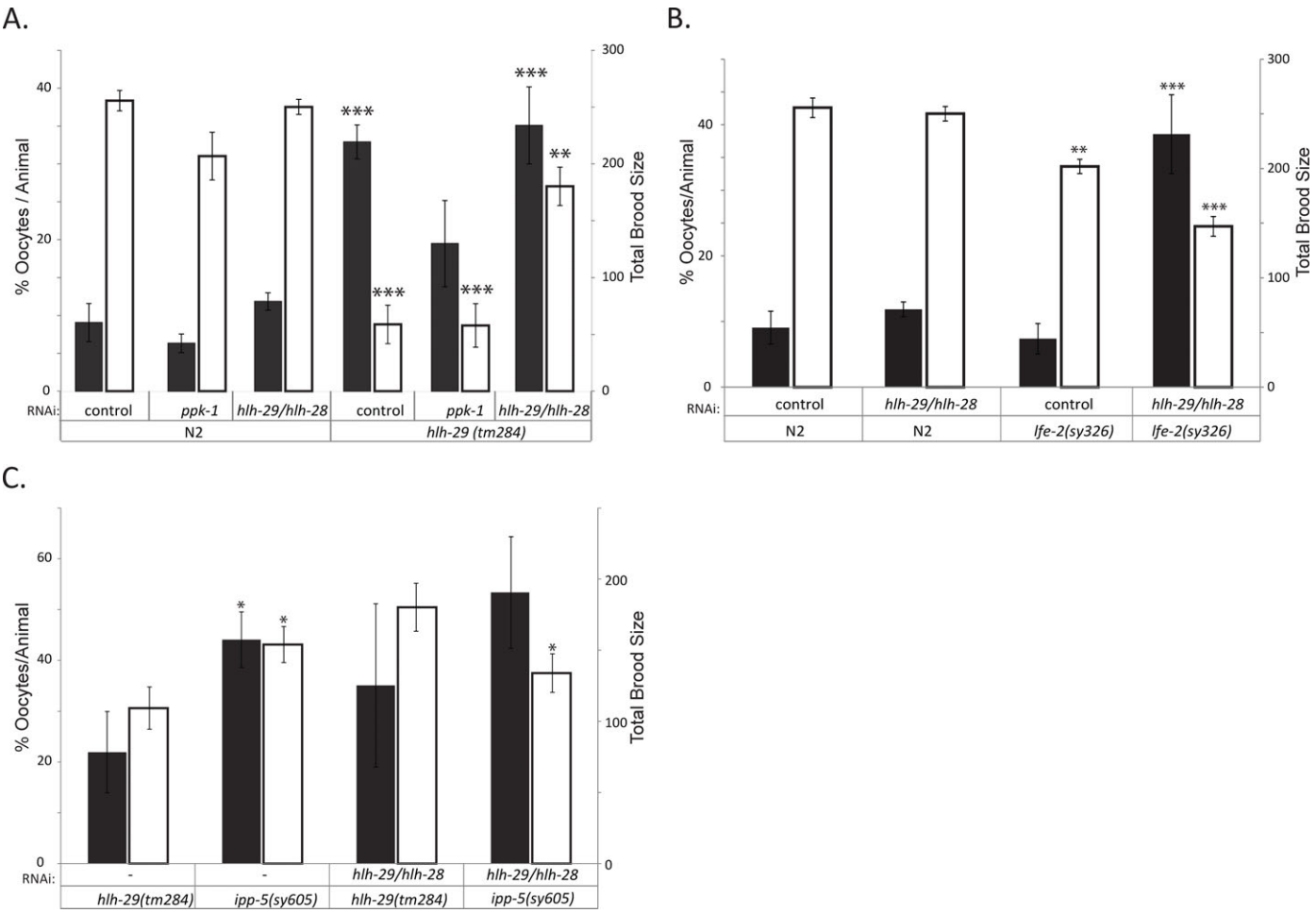

Fig. 4. Genetic interactions between hlh-29 and selected IP3 signaling genes. (A) Genetic interactions between *hlh-29* and *ppk-1*. **(B)** Genetic interactions between *hlh-29* and *lfe-2*. **(C)** Genetic interactions between *hlh-29* and *ipp-5*. Dark bars represent the percentage of oocytes (unfertilized) laid on plates out of the total number of viable, fertilized eggs and unfertilized oocytes. Not included in these numbers were irregularly shaped, inviable eggs and egg fragments. White bars represent the total brood size, or absolute number of viable, fertilized eggs. Data represent the mean of three experiments, error bars represent standard error of the mean, *N* was equal to ten, and significance was determined using single factor ANOVA. All animals were compared to N2 eating control RNAi, except in C where *ipp-5* animals were compared to *hlh-29(tm284)* animals under the same RNAi conditions. * P-value <0.05; ** P-value <0.005; *** P-value <0.0005.

throughout their egg-laying period and laid a significantly higher percentage than wild-type animals. This phenotype was suppressed by *ppk-1* RNAi (Fig. 4A), indicating that *ppk-1* is epistatic to *hlh-29*, and further supporting our molecular finding that *hlh-29* acts upstream of *ppk-1*.

The enzymes IP_3 kinase, encoded by *lfe-2*, and inositol polyphosphate 5-phosphatase, encoded by *ipp-5*, function to reduce the intracellular levels of IP_3 (Clandinin et al., 1998; Bui and Sternberg, 2002). Loss of either IPP-5 or LFE-2 effectively increases IP_3 levels, but results in only moderate ovulation defects. *ipp-5* animals produce fewer progeny than wild-type animals and lay unfertilized oocytes because of a hyperactive distal spermatheca valve (Bui and Sternberg, 2002). *lfe-2* animals also have small brood sizes, but no other ovulation defects are evident (Clandinin et al., 1998). Interestingly, animals that carry loss-of-function alleles in both *ipp-5* and *lfe-2*, and animals that over-express *lfe-2* are sterile. In the latter case, sterility is caused by failure of the spermatheca-uterine valve to open (Clandinin et al., 1998), a phenotype very similar to the ovulation defect of *hlh-29(tm284)/+ hlh-29/hlh-28*(RNAi) animals and in support of slightly increased *lfe-2* activity in *hlh-29(tm284)* animals. In our genetic interaction studies, *lfe-2(sy36)*; *hlh-29/hlh-28*(RNAi) animals and *ipp-5(sy605)*; *hlh-29/hlh-28*(RNAi) animals laid a significantly higher percentage of unfertilized oocytes than either wild-type or single mutant animals (Fig. 3B,C). Additionally, brood sizes were significantly reduced in *hlh-29(tm284)*, *ipp-5(sy605)*, and *lfe-2(sy36)* animals when compared to wild-type, and were reduced further in *ipp-5(sy605)*; *hlh-29/hlh-28*(RNAi) and *lfe-2(sy36)*;*hlh-29/hlh-28*(RNAi) animals. These results show genetic interactions between *hlh-29* and *ipp-5* and between *hlh-29* and *lfe-2*, and we suggest that they are representative of the phenotypes that would be expected in either *lfe-2*(gain-of-function); *ipp-5*(loss-of-function) or *lfe-2*(loss-of-function); *ipp-5*(gain-of-function) animals.

The percentage of unfertilized oocytes in *hlh-29(tm284)* animals does not change significantly upon treatment with *hlh-29/hlh-28* RNAi, suggesting that HLH-29 and HLH-28 do not function redundantly to control ovulation (Fig. 4A). Interestingly, the brood size data contradicts this interpretation, as *hlh-29(tm284)* animals show significantly larger brood sizes after treatment with *hlh-29/hlh-28* RNAi. One possibility for this discrepancy would be that RNAi artificially induces egg-laying via a process that is independent of HLH-29 and HLH-28. We do

not believe this explanation is plausible, however, because brood size was not increased in *hlh-29(tm284)* animals subjected to control RNAi when compared to those that were untreated with RNAi (compare Fig. 4A to Fig. 4C). We suggest that this result and the *fog-2(q71)*; *hlh-29/hlh-28* (RNAi) results presented above are indicative of a separate function for HLH-28 in controlling ovulation events upstream of spermatheca entry and exit.

HLH-29 and HLH-28 affect the morphology of the gonad arm

As mentioned above, animals that are homozygous for *hlh-29(tm284)* show variably abnormal morphological defects of the somatic gonad which became more pronounced when animals were cultured at higher temperatures. Because our data showed that *hlh-29/hlh-28* RNAi can rescue the brood size phenotype of *hlh-29(tm284)* animals, we expected that the gonad morphology defects would also be rescued. Surprisingly, gonad defects were more pronounced in *hlh-29/hlh-28* RNAi treated *hlh-29(tm284)* animals than in untreated animals, though the phenotype was still variably expressed and incompletely penetrant. Supplementary material Fig. S2D,E shows an animal representative of the morphology defects seen in some *hlh-29(tm284) hlh-29/hlh-28(RNAi)* animals. To identify genes that may be targeted by either HLH-29 or HLH-28 during gonad development, and to determine if HLH-28 and HLH-29 may be jointly regulating expression of those genes, we compared the activities of the IP_3 signaling genes and the activities of six other genes whose expression overlapped with *hlh-29* in at least two tissues and that were previously shown to affect reproduction (supplementary material Table S1A) in *hlh-29(tm284)* and *hlh-29(tm284)* animals treated with *hlh-29/hlh-28*(RNAi). The expression of five of these genes was affected in *hlh-29(tm284)* animals (supplementary material Table S1B). These genes and the proteins they encode are: *nhr-6*, a NR4A nuclear receptor protein required for spermatheca development (Heard et al., 2010); *emb-9*, a Type IV basement membrane collagen required for embryonic morphogenesis (Guo et al., 1991); *sca-1*, a calcium transporting ATPase that is predicted to interact with the IP_3 receptor protein, ITR-1 (Nehrke et al., 2008); and two genes required for gonadal morphogenesis, *mig-6*, an extracellular matrix protein (Kawano et al., 2009) and *pyp-1*, nucleosome remodeling factor (Ko et al., 2007). We found that the expression of *sca-1*, *nhr-6*, *emb-9*, and most of the IP_3 signaling genes was similarly affected in RNAi treated animals; however, the expression of *pyp-1*, *mig-6*, and the IP_3 signaling pathway gene *let-23*, was affected differently in RNAi treated *hlh-29(tm284)* animals (supplementary material Table S1C). Altogether, these results suggest that both HLH-28 and HLH-29 are required for normal development of the somatic gonad.

Conclusions

Our molecular and genetic data indicate that HLH-29 acts in both the distal spermatheca valve and the spermatheca-uterine valve to regulate ovulation by mediating IP_3 signaling (Fig. 3B). Previous studies have identified bHLH proteins as regulators of the IP_3 receptor genes in mice (Konishi et al., 1999) and in yeast (Shetty and Lopes, 2010); however, this is the first to show coordinated regulation of multiple genes within the IP_3 signaling pathway. HLH-29 is a member of the *C. elegans* REF-1 family, functional homologs of HES proteins (Neves and Priess, 2005). Our results, then, are one of the first to demonstrate the involvement of a HES protein in the modification and regulation of an adult phenotype and a possible link between IP_3 and Notch signaling in this organism. These results also underscore the importance of tight regulation of the IP_3 signaling cascade, and demonstrate how IP_3 signaling can be modulated at multiple inputs in the pathway. Previous results show that perturbing any of the genes in this pathway can have moderate to severe effects on ovulation. HLH-29 seems to act to increase the levels of IP_3, either by activating the *ppk-1* gene, or by repressing *lfe-2* and *ipp-5*, two genes needed to reduce intracellular levels of IP_3. Our gene expression data also suggest that HLH-29 represses the gene for phospholipase C ε, *plc-1*. This result contradicts our genetic data, which strongly correlate with ovulation phenotypes seen in *plc-1* loss of function mutants. One plausible explanation is that the expression levels reported here are indicative of HLH-29 dependent regulation of *plc-1* levels in cells outside of the spermatheca. Finally, our results indicate that HLH-29 regulates genes required for the development of the spermatheca and of the somatic gonad, and are particularly exciting in that they underscore the ability of HES proteins to regulate tissue morphology and organ development in larval and adult animals. This study did not directly address the possible roles of HLH-28 in reproduction; however, treating either *fog-2* animals or *hlh-29* animals with *hlh-29/hlh-28* RNAi increased the total number of ovulation events in both strains. These results suggest that HLH-28 may negatively regulate ovulation separately from HLH-29.

Acknowledgements

We gratefully acknowledge Drs. W.W. Walthall, M. Zellars, and R. Kohn for helpful advice; undergraduate research assistant Stephanie Pritchett for performing brood size assays at 16℃ and 20℃ and the Caenorhabditis Genetics Center for providing strains. While performing these studies A. White and S. Pritchett were Biotech Scholars, supported by Howard Hughes Medical Institute, Division of Undergraduate Education, Grant #52005875. This research and undergraduate student researcher A. Fearon were supported by National Science Foundation grant #MCB0919413 to C. Johnson.

References

Axelson, H. (2004). The Notch signaling cascade in neuroblastoma: role of the basic helix-loop-helix proteins HASH-1 and HES-1. *Cancer Lett.* **204**, 171-178.

Ballow, D., Meistrich, M. L., Matzuk, M. and Rajkovic, A. (2006). Sohlh1 is essential for spermatogonial differentiation. *Dev. Biol.* **294**, 161-167.

Barnes, R. M. and Firulli, A. B. (2009). A twist of insight - the role of Twist-family bHLH factors in development. *Int. J. Dev. Biol.* **53**, 909-924.

Bitra, K., Tan, A., Dowling, A. and Palli, S. R. (2009). Functional characterization of PAS and HES family bHLH transcription factors during the metamorphosis of the red flour beetle, Tribolium castaneum. *Gene* **448**, 74-87.

Brenner, S. (1974). The genetics of *Caenorhabditis elegans*. *Genetics* **77**, 71-94.

Broitman-Maduro, G., Maduro, M. F. and Rothman, J. H. (2005). The noncanonical binding site of the MED-1 GATA factor defines differentially regulated target genes in the *C. elegans* mesendoderm. *Dev. Cell* **8**, 427-433.

Bui, Y. K. and Sternberg, P. W. (2002). *Caenorhabditis elegans* inositol 5-phosphatase homolog negatively regulates inositol 1, 4, 5-triphosphate signaling in ovulation. *Mol. Biol. Cell* **13**, 1641-1651.

Clandinin, T. R., DeModena, J. A. and Sternberg, P. W. (1998). Inositol trisphosphate mediates a RAS-independent response to LET-23 receptor tyrosine kinase activation in *C. elegans*. *Cell* **92**, 523-533.

Du, Y. and Yip, H. K. (2011). The expression and roles of inhibitor of DNA binding helix-loop-helix proteins in the developing and adult mouse retin. *Neuroscience* **175**, 367-379.

Egoz-Matia, N., Nachman, A., Halachmi, N., Toder, M., Klein, Y. and Salzberg, A. (2011). Spatial regulation of cell adhesion in the Drosophila wing is mediated by Delilah, a potent activator of betaPS integrin expression. *Dev. Biol.* **351**, 99-109.

Felton, C. M. and Johnson, C. M. (2011). Modulation of dopamine-dependent behaviors by the *Caenorhabditis elegans* Olig homolog HLH-17. *J. Neurosci. Res.* **89**, 1627-1636.

Fischer, A. and Gessler, M. (2007). Delta-Notch--and then? Protein interactions and proposed modes of repression by Hes and Hey bHLH factors. *Nucleic Acids Res.* **35**, 4583-4596.

Fischer, A., Schumacher, N., Maier, M., Sendtner, M. and Gessler, M. (2004). The Notch target genes Hey1 and Hey2 are required for embryonic vascular development. *Genes Dev.* **18**, 901-911.

Govindan, J. A., Cheng, H., Harris, J. E. and Greenstein, D. (2006). Galphao/i and Galphas signaling function in parallel with the MSP/Eph receptor to control meiotic diapause in *C. elegans*. *Curr. Biol.* **16**, 1257-1268.

Govindan, J. A., Nadarajan, S., Kim, S., Starich, T. A. and Greenstein, D. (2009). Somatic cAMP signaling regulates MSP-dependent oocyte growth and meiotic maturation in *C. elegans*. *Development* **136**, 2211-2221.

Greenstein, D. (2005). Control of oocyte meiotic maturation and fertilization. *WormBook.* **1-12**.

Guo, X. D., Johnson, J. J. and Kramer, J. M. (1991). Embryonic lethality caused by mutation in basement membrane collagen of *C. elegans*. *Nature* **349**, 707-709.

Han, S. M., Cottee, P. A. and Miller, M. A. (2010). Sperm and oocyte communication mechanisms controlling *C. elegans* fertility. *Dev. Dyn.* **239**, 1265-1281.

Hartman, J., Lam, E. W., Gustafsson, J. A. and Strom, A. (2009). Hes-6, an inhibitor of Hes-1, is regulated by 17beta-estradiol and promotes breast cancer cell proliferation. *Breast Cancer Res.* **11**, R79.

Heard, M., Maina, C. V., Morehead, B. E., Hoener, M. C., Nguyen, T. Q., Williams, C. C., Rowan, B. G. and Gissendanner, C. R. (2010). A functional NR4A nuclear receptor DNA-binding domain is required for organ development in *Caenorhabditis elegans*. *Genesis* **48**, 485-491.

Hoogewijs, D., Houthoofd, K., Matthijssens, F., Vandesompele, J. and Vanfleteren, J. R. (2008). Selection and validation of a set of reliable reference genes for quantitative sod gene expression analysis in *C. elegans*. *BMC Mol. Biol.* **9**, 9.

Iwasaki, K., McCarter, J., Francis, R. and Schedl, T. (1996). emo-1, a *Caenorhabditis elegans* Sec61p g homologue, is required for oocyte development and ovulation. *J. Cell Biol.* **134**, 699-714.

Kageyama, R., Ohtsuka, T. and Kobayashi, T. (2007). The Hes gene family: repressors and oscillators that orchestrate embryogenesis. *Development* **134**, 1243-1251.

Kageyama, R., Ohtsuka, T. and Kobayashi, T. (2008). Roles of Hes genes in neural development. *Dev. Growth Differ.* **50** Suppl 1:, S97-S103.

Kamath, R. S. and Ahringer, J. (2003). Genome-wide RNAi screening in *Caenorhabditis elegans*. *Methods* **30**, 313-321.

Kawano, T., Zheng, H., Merz, D. C., Kohara, Y., Tamai, K. K., Nishiwaki, K. and Culotti, J. G. (2009). *C. elegans* mig-6 encodes papilin isoforms that affect distinct aspects of DTC migration, and interacts genetically with mig-17 and collagen IV. *Development* **136**, 1433-1442.

Ko, K. M., Lee, W., Yu, J. R. and Ahnn, J. (2007). PYP-1, inorganic pyrophosphatase, is required for larval development and intestinal function in *C. elegans*. *FEBS Lett.* **581**, 5445-5453.

Konishi, Y., Ohkawa, N., Makino, Y., Ohkubo, H., Kageyama, R., Furuichi, T., Mikoshiba, K. and Tamura, T. (1999). Transcriptional regulation of mouse type 1 inositol 1,4,5-trisphosphate receptor gene by NeuroD-related factor. *J. Neurochem.* **72**, 1717-1724.

Lewis, J. A. and Fleming, J. T. (1995). Basic culture methods. In *Caenorhabditis elegans, Modern Biological Analysis of an Organism* (ed. H. F. Epstein and D. C. Shakes). San Diego: Academic Press.

Li, F., Guo, S., Zhao, Y., Chen, D., Chong, K. and Xu, Y. (2010). Overexpression of a homopeptide repeat-containing bHLH protein gene (OrbHLH001) from Dongxiang Wild Rice confers freezing and salt tolerance in transgenic Arabidopsis. *Plant Cell Rep.* **29**, 977-986.

Li, S., Mark, S., Radde-Gallwitz, K., Schlisner, R., Chin, M. T. and Chen, P. (2008). Hey2 functions in parallel with Hes1 and Hes5 for mammalian auditory sensory organ development. *BMC Dev. Biol.* **8**, 20.

Ligon, K. L., Fancy, S. P., Franklin, R. J. and Rowitch, D. H. (2006). Olig gene function in CNS development and disease. *Glia* **54**, 1-10.

Lo, P. C., Zaffran, S., Senatore, S. and Frasch, M. (2007). The Drosophila Hand gene is required for remodeling of the developing adult heart and midgut during metamorphosis. *Dev. Biol.* **311**, 287-296.

Long, T. A., Tsukagoshi, H., Busch, W., Lahner, B., Salt, D. E. and Benfey, P. N. (2010). The bHLH transcription factor POPEYE regulates response to iron deficiency in Arabidopsis roots. *Plant Cell* **22**, 2219-2236.

Lu, H., Kozhina, E., Mahadevaraju, S., Yang, D., Avila, F. W. and Erickson, J. W. (2008). Maternal Groucho and bHLH repressors amplify the dose-sensitive X chromosome signal in Drosophila sex determination. *Dev. Biol.* **323**, 248-260.

Lu, J. P., Zhang, J., Kim, K., Case, T. C., Matusik, R. J., Chen, Y. H., Wolfe, M., Nopparat, J. and Lu, Q. (2010). Human homolog of Drosophila Hairy and enhancer of split 1, Hes1, negatively regulates delta-catenin (CTNND2). expression in cooperation with E2F1 in prostate cancer. *Mol. Cancer* **9**, 304.

Maroto, M., Iimura, T., Dale, J. K. and Bessho, Y. (2008). BHLH proteins and their role in somitogenesis. *Adv. Exp. Med. Biol.* **638**, 124-139.

McCarter, J., Bartlett, B., Dang, T. and Schedl, T. (1999). On the control of oocyte meiotic maturation and ovulation in *Caenorhabditis elegans*. *Dev. Biol.* **205**, 111-128.

McMiller, T. L., Sims, D., Lee, T., Williams, T. and Johnson, C. M. (2007). Molecular characterization of the *Caenorhabditis elegans* REF-1 family member, hlh-29/hlh-28. *Biochim. Biophys. Acta* **1769**, 5-19.

Nasgashio, R., Sato, Y., Matsumoto, T., Kageyama, T., Hattori, M., Iyoda, A., Satoh, Y., Ryuge, S., Masuda, N., Jiang, S. X. et al. (2011). The balance between the expressions of hASH1 and HES1 differs between large cell neuroendocrine carcinoma and small cell carcinoma of the lung. *Lung Cancer* **74**, 405-410.

Nehrke, K., Denton, J. and Mowrey, W. (2008). Intestinal Ca2+ wave dynamics in freely moving *C. elegans* coordinate execution of a rhythmic motor program. *Am. J. Physiol. Cell Physiol.* **294**, C333-C344.

Neves, A. and Priess, J. R. (2005). The REF-1 family of bHLH transcription factors pattern *C. elegans* embryos through Notch-dependent and Notch-independent pathways. *Dev. Cell* **8**, 867-879.

Parthasarathy, R., Tan, A. and Palli, S. R. (2008). bHLH-PAS family transcription factor methoprene-tolerant plays a key role in JH action in preventing the premature development of adult structures during larval-pupal metamorphosis. *Mech. Dev.* **125**, 601-616.

Pin, C. L., Rukstalis, J. M., Johnson, C. and Konieczny, S. F. (2001). The bHLH transcription factor Mist1 is required to maintain exocrine pancreas cell organization and acinar cell identity. *J. Cell Biol.* **155**, 519-530.

Shetty, A. and Lopes, J. M. (2010). Derepression of INO1 transcription requires cooperation between the Ino2p-Ino4p heterodimer and Cbf1p and recruitment of the ISW2 chromatin-remodeling complex. *Eukaryot. Cell* **9**, 1845-1855.

Sparrow, D. B., Guillen-Navarro, E., Fatkin, D. and Dunwoodie, S. L. (2008). Mutation of Hairy-and-Enhancer-of-Split-7 in humans causes spondylocostal dysostosis. *Hum. Mol. Genet.* **17**, 3761-3766.

Sparrow, D. B., Sillence, D., Wouters, M. A., Turnpenny, P. D. and Dunwoodie, S. L. (2010). Two novel missense mutations in HAIRY-AND-ENHANCER-OF-SPLIT-7 in a family with spondylocostal dysostosis. *Eur. J. Hum. Genet.* **18**, 674-679.

Stockhausen, M. T., Sjolund, J. and Axelson, H. (2005). Regulation of the Notch target gene Hes-1 by TGFalpha induced Ras/MAPK signaling in human neuroblastoma cells. *Exp. Cell Res.* **310**, 218-228.

Van Wayenbergh, R., Taelman, V., Pichon, B., Fischer, A., Kricha, S., Gessler, M., Christophe, D. and Bellefroid, E. J. (2003). Identification of BOIP, a novel cDNA highly expressed during spermatogenesis that encodes a protein interacting with the orange domain of the hairy-related transcription factor HRT1/Hey1 in Xenopus and mouse. *Dev. Dyn.* **228**, 716-725.

Webb, K. J., Coolen, M., Gloeckner, C. J., Stigloher, C., Bahn, B., Topp, S., Ueffing, M. and Bally-Cuif, L. (2011). The Enhancer of split transcription factor Her8a is a novel dimerisation partner for Her3 that controls anterior hindbrain neurogenesis in zebrafish. *BMC Dev. Biol.* **11**, 27.

Wiese, C., Heisig, J. and Gessler, M. (2010). Hey bHLH factors in cardiovascular development. *Pediatr. Cardiol.* **31**, 363-370.

Xin, M., Small, E. M., van Rooij, E., Qi, X., Richardson, J. A., Srivastava, D., Nakagawa, O. and Olson, E. N. (2007). Essential roles of the bHLH transcription factor Hrt2 in repression of atrial gene expression and maintenance of postnatal cardiac function. *Proc. Natl. Acad. Sci. USA* **104**, 7975-7980.

Xu, X., Guo, H., Wycuff, D. L. and Lee, M. (2007). Role of phosphatidylinositol-4-phosphate 5′ kinase (ppk-1). in ovulation of *Caenorhabditis elegans*. *Exp. Cell Res.* **313**, 2465-2475.

Yin, X., Gower, N. J., Baylis, H. A. and Strange, K. (2004). Inositol 1,4,5-trisphosphate signaling regulates rhythmic contractile activity of myoepithelial sheath cells in *Caenorhabditis elegans*. *Mol. Biol. Cell* **15**, 3938-3949.

Zhao, Y., Johansson, C., Tran, T., Bettencourt, R., Itahana, Y., Desprez, P. Y. and Konieczny, S. F. (2006). Identification of a basic helix-loop-helix transcription factor expressed in mammary gland alveolar cells and required for maintenance of the differentiated state. *Mol. Endocrinol.* **20**, 2187-2198.

Zhou, J., Li, F., Wang, J. L., Ma, Y., Chong, K. and Xu, Y. Y. (2009). Basic helix-loop-helix transcription factor from wild rice (OrbHLH2) improves tolerance to salt- and osmotic stress in Arabidopsis. *J. Plant Physiol.* **166**, 1296-1306.